Arch. Metall. Mater. **65** (2020), 1, 125-131

DOI: 10.24425/amm.2019.131105

MAGDALENE EDET IKPI[1*], FIDELIS EBUNTA ABENG[2]

ELECTROCHEMICAL AND QUANTUM CHEMICAL INVESTIGATION ON ADSORPTION OF NIFEDIPINE AS CORROSION INHIBITOR AT API 5L X-52 STEEL / HCL ACID INTERFACE

Nifedipine, a pyridine derivative was investigated as corrosion inhibitor for API 5L X-52 steel in 2 M HCl solution by potentiodynamic polarization, electrochemical impedance spectroscopy and quantum chemical calculations. Statistical tools were used to compare results of the experimental methods. The results showed that nifedipine is capable of inhibiting the corrosion of API 5L X-52 steel in 2 M HCl solution. Potentiodynamic polarization results reveal that nifedipine functions as a mixed-type inhibitor and presents an inhibition efficiency of about 78% at 500 ppm. Impedance data reveal an increasing charge transfer resistance with increasing inhibitor concentration and also shows comparable inhibition efficiency of about 89-94% at 500 ppm. Thermodynamic parameters imply that nifedipine is adsorbed on the steel surface by a physiochemical process and obeys Langmuir adsorption isotherm. The calculated molecular properties namely the highest occupied molecular orbital energy, lowest unoccupied molecular orbital energy, chemical hardness, energy gap, dipole moment, electronegativity and global nucleophilicity index all show a positive relationship to the observed corrosion inhibition efficiency.

Keywords: Nifedipine, corrosion inhibition, electrochemical impedance, carbon steel, quantum chemical study

1. Introduction

The problem of metal corrosion in acid medium is a severe environmental set back in the field of oil and gas, fertilizer, metallurgical and other manufacturing industries. The industrial cost involved in preventing the problems of corrosion is enormous and so there is a significant effort from industries to find inexpensive and efficient additives to control corrosion. Medicinal drugs are gradually emerging as promising candidates in their application as corrosion inhibitors chiefly due to their natural origin [1], non-toxicity [2] and eco-friendly attributes. The study utilizes a pharmaceutical drug, nifedipine, which has no established adverse toxicological and ecological effect on the environment [3-5]. A review [6] detailing most of the contributions made to literature on the use of pharmaceutical drugs as corrosion inhibitors reveals that their effectiveness depends on their chemical composition, molecular structure and affinities for the metal surface. These substances contain reactive sites like oxygen, nitrogen and/or sulphur atoms having lone pairs of electrons and aromatic rings with delocalized π electrons that support their adsorption onto metal surfaces thus preventing corrosion. Furthermore, the author opines that the mechanism controlling the corrosion inhibition of drugs on various metal surfaces still requires sufficient research both experimentally and theoretically to substantiate any mechanism. Morad et al. [7] reported a study on cefatrexyl in the corrosion inhibition of iron in chloride, sulphate and phosphate media using polarization and electrochemical impedance spectroscopy methods. The author proposed that the formation of soluble Fe(II)-cefatrexyl-Cl complex was responsible for the low inhibition performance of cefatrexyl in chloride solution and claimed that the compound adsorbed through the outer surface of iron by the formation of adsorbed ion pairs. Eddy et al. [8,9] in their work on the inhibitory action of penicillin proposed that physical adsorption of the compound onto the mild steel surface was via weak intermolecular interactions and that the strength of interaction between penicillin and steel surface is always variable and dependent on adsorption active centers. The adsorption and inhibitive effect of ceftezole for the corrosion of mild steel in HCl solution was reported by Singh and Ebenso [10] employing weight loss, electrochemical impedance spectroscopy and Tafel polarization techniques. The results showed an increase in inhibition efficiency with increase in inhibitor concentration and temperature. Potentiodynamic polarization results gave evidence of a mixed type inhibitor

[1] UNIVERSITY OF CALABAR, CORROSION AND ELECTROCHEMISTRY RESEARCH LABORATORY, DEPARTMENT OF PURE AND APPLIED CHEMISTRY, CALABAR-NIGERIA
[2] CROSS RIVER UNIVERSITY OF TECHNOLOGY, MATERIALS AND ELECTROCHEMISTRY RESEARCH GROUP, DEPARTMENT OF CHEMISTRY, CALABAR-NIGERIA

* Corresponding author: meikpi@unical.edu.ng, me_ikpi@yahoo.com

of its function and Langmuir adsorption isotherm was obeyed. The significance of the present study is based on the premise that corrosion inhibition and protection of metals or alloys play important role in chemical industries of any economy. Therefore this paper seeks to evaluate the potential of nifedipine, a pharmaceutical drug, as a suitable alternative to highly expensive and toxic corrosion inhibitors, using experimental and quantum chemical approaches.

2. Experimental

2.1. Materials

The API 5L X-52 steel specimen was taken from a portion of a carbon steel pipeline with chemical composition in weight % as follows; C(0.22), Mn(1.40), Si(0.45), P(0.025), S(0.015), Cr(0.20), Ni(0.20), Ti(0.04), Nb(0.15), Mo(0.08), V(0.15), Al(0.030) and the balance Fe [11]. Nifedipine was obtained from Peace Land Pharmaceutical shop, Ndidem Usang Iso Road Calabar-Nigeria. All reagents were of analar grade. The steel samples were cut into dimensions of about (1×1×1) cm^3, ground and polished using SiC paper up to #2000 grit size. These were mounted using epoxy resin with 1 cm^2 surface area exposed. Further preparation of the steel surface entailed polishing, cleaning with distilled water and acetone and drying in cool air.

2.2. Preparation of inhibitor stock solution and electrochemical measurements

The inhibitor solution was prepared as previously described [12]. A GAMRY Reference 600 potentiostat was used for the electrochemical measurements and controlled with Gamry Framework software. The analysis of the polarization and impedance curves was done using Echem Analyst software. A three-electrode electrolytic cell was utilized with a Pt plate as the auxiliary electrode, a saturated calomel electrode (SCE) as the reference electrode and the steel sample as the working electrode. Potentiodynamic polarization measurements were obtained at a potential range of –250 mV/SCE with respect to the open circuit potential (OCP) to 600 mV/SCE above OCP, with scanning rate of 0.5 mV/s. Electrochemical Impedance Spectroscopy (EIS) measurements were carried out at a frequency range of 10^5 to 5×10^{-2} Hz and with a signal amplitude perturbation of 10 mV. All experiments were conducted at room temperature of 30°C.

2.3. Theoretical approach

Simulations were done by Density Functional Theory (DFT) electronic program $Dmol^{-1}$ using Material Studio 4.0 software, in combination with the B3LYP functional. DFT/ B3LYP is known to produce good estimates of molecular properties that are related to molecular reactivity [13]. The molecular properties that are obtained by DFT/ B3LYP include the energy of highest occupied molecular orbital (E_{HOMO}), energy of the lowest unoccupied molecular orbital (E_{LUMO}), ionization potential (IP), electron affinity (EA), electronegativity (χ), global hardness (η), global softness (σ) and dipole moment (μ). Obi-Egbedi *et al*., [14], defined these quantities based on Koopman's theorem. The values of the total electronic energy gives the IP and EA of the inhibitor. The ionization potential Eq. (1) and electron affinity Eq. (2) are related to the E_{HOMO} and E_{LUMO} respectively. Energy gap ΔE, can be calculated as illustrated in Eq. (3).

$$IP = -E_{HOMO} \tag{1}$$

$$EA = -E_{LUMO} \tag{2}$$

$$\Delta E = E_{LUMO} - E_{HOMO} \tag{3}$$

The parameter, global hardness η Eq. (4) measures the resistance of the atom to transfer charge whereas global softness σ describes the capacity of an atom or group of atom to receive electrons. It is estimated as the reciprocal of global hardness (Eq. (5)) [13].

$$\eta = -\frac{1}{2}\left(E_{HOMO} - E_{LUMO}\right) \tag{4}$$

$$\sigma = 1/\eta \tag{5}$$

The global electrophilicity index ω is always estimated by using the electronegativity and chemical hardness parameters as given in Eq. (6).

$$\omega = \frac{\chi^2}{2\eta} \tag{6}$$

A high value of electrophilicity describes a good electrophile while low electrophilicity value describes a good nucleophile. Electronegativity gives the power of an electron or group of atoms to attract electrons towards itself. According to Koopman's theorem, electronegativity can be estimated using Eq. (7).

$$\chi = -\frac{1}{2}\left(E_{HOMO} + E_{LUMO}\right) \tag{7}$$

The fraction of electrons transferred δ is usually evaluated following Eq. (8);

$$\delta = \frac{\chi_{\mathrm{Fe}} - \chi_{inh}}{2\left(\eta_{\mathrm{Fe}} + \eta_{inh}\right)} \tag{8}$$

where χ_{Fe} and χ_{inh} are the electronegativity values of Fe and inhibitor respectively while η_{Fe} and η_{inh} are the global hardness of Fe and inhibitor respectively. The values of χ_{Fe} and η_{Fe} are considered as 7 $eVmol^{-1}$ and 0 $eVmol^{-1}$ respectively [15]. From the simplest molecular orbital theory model, additional electrons would occupy the lowest unoccupied molecular orbital (LUMO) and ionization electrons would be removed from the highest occupied molecular orbital (HOMO).

3. Results and discussion

3.1. Potentiodynamic polarization curves

The potentiodynamic polarization curves for API 5L X-52 steel in 2 M HCl solution at 303 K in the absence and presence of different concentrations of the inhibitor are given in the Tafel plots of Fig. 1. Corrosion current densities I_{corr}, corrosion potentials E_{corr}, anodic and cathodic Tafel slopes (β_a and β_c respectively) were obtained from the Tafel plots using Echem Analyst software and are listed in Table 1. The surface coverage θ and inhibition efficiency IE was calculated by applying Eq. (9) and Eq. (10);

$$\theta = \frac{I_{corr}(blank) - I_{corr}(inh)}{I_{corr}(blank)} \tag{9}$$

$$IE = \frac{I_{corr}(blank) - I_{corr}(inh)}{I_{corr}(blank)} \times 100 \tag{10}$$

where $I_{corr}(blank)$ and $I_{corr}(inh)$ are the corrosion current densities in the absence and presence of inhibitor respectively.

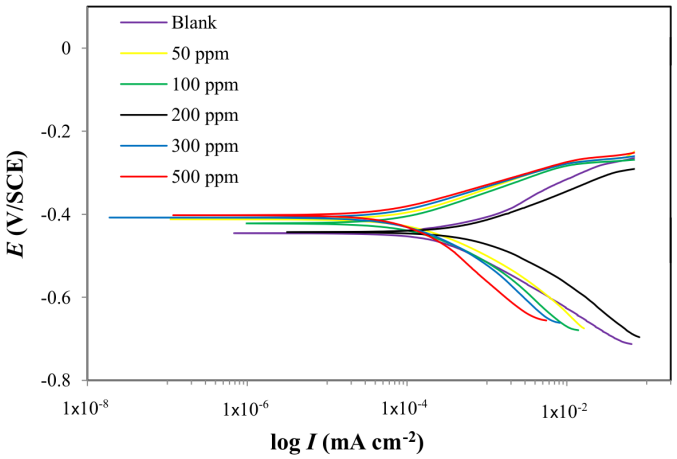

Fig. 1. Potentiodynamic polarization curves for API 5L X-52 steel in 2 M HCl solution in the absence and presence of different concentrations of nifedipine at 303 K

TABLE 1

Tafel polarization parameters for API 5L X-52 steel in the absence and presence of different concentrations of nifedipine at 303 K

Inhibitor conc. (ppm)	E_{corr} (mV)	β_a (mV dec^{-1})	β_c (mV dec^{-1})	I_{corr} (μA cm^{-2})	Surface coverage θ	IE (%)
Blank	–446	102.3	454.2	560		
50	–445	112.7	95.6	392	0.3000	30.0
100	–430	92.8	119.9	361	0.3553	35.5
200	–445	74.3	117.2	291	0.4830	48.3
300	–439	83.0	156.1	248	0.5571	55.7
500	–440	78.2	83.7	125	0.7767	77.7

Only the cathodic slopes changed significantly compared to the reference sample indicating more inhibitory effect on cathodic sites. In addition it was observed that the anodic β_a and cathodic β_c slopes of the inhibitor solutions affect both reactions [16]. Generally, an inhibitor is said to be anodic or cathodic type if the displacement in the corrosion potential E_{corr} of the inhibitor against the blank is greater than 85 mV while if the shift is less than 85 mV it can be regarded as mixed type [17]. In the present study, the inhibitor causes a minor change in E_{corr} value with respect to the blank with a maximum displacement of 16 mV. The results suggests that the inhibitor acted as a mixed type inhibitor.

I_{corr} values show a progressive decrease with increasing inhibitor concentration and a corresponding increase in inhibition efficiency. The result is reflective of the adsorption of inhibitor molecules at the steel surface [18].

3.2. Electrochemical impedance spectroscopy curves

Impedance measurements were carried out at 303 K after 30 minutes of immersion in 2 M HCl solution in the absence and presence of different concentrations of the inhibitor as shown in the Nyquist plots of Fig. 2. The capacitive loops are characterized by depressed semicircles and with increasing diameters as the concentration of the inhibitor increases. This shows that the inhibitor molecules provide increasing corrosion protection at the metal-solution interface. An equivalent circuit was proposed to fit the impedance spectra for the analysis of the impedance characteristics as shown in Fig. 3. The model considers a film resistance R_f arising from the inhibitor molecule film adsorbed on the steel surface, a constant phase element (CPE) Q_f associated with the adsorbed film, a charge-transfer resistance R_{ct}, a constant phase double layer Q_{dl} and the solution resistance R_s. The impedance values obtained from the fit are presented in Table 2. Alternatively, the charge-transfer resistance could be obtained from the difference in impedance at low and high frequencies as suggested by Chami et al. [16] and denoted here as R'_{ct}. The double layer capacitance (C_{dl}) values were calculated from the frequency at which the imaginary of the impedance is maximal ($-Z_{max}$) using Eq. (11).

$$C_{dl} = \frac{1}{2\pi f_{max} R_{ct}} \tag{11}$$

The percentage inhibition efficiency based on charge-transfer resistance values was calculated using Eq. (12) and given in TABLE 2 as IE and IE' depending on the determination of the charge-transfer values.

$$IE = \left[1 - \frac{R_{ct}(blank)}{R_{ct}(inh)}\right] \times 100 \tag{12}$$

where $R_{ct}(inh)$ and $R_{ct}(blank)$ are the charge transfer resistance with and without the addition of inhibitor respectively. The results in Table 2 reveal a general increase in R_{ct} and R'_{ct} values and decrease in Q_{dl} and C_{dl} values as the concentration of inhibitor increases. Both IE and IE' have comparable values and the

increase with increasing inhibitor concentration indicates that corrosion of API 5L X-52 steel in 2 M HCl solution is restricted by a charge-transfer process [16,19]. The decrease in Q_{dl} and C_{dl} values reflects an increase in the thickness of the electrical double layer as a result of the adsorption of the inhibitor molecules at the steel surface/solution interface. The film of adsorbed inhibitor molecules provides a barrier which prevents the corrosion process leading to an increased inhibition efficiency.

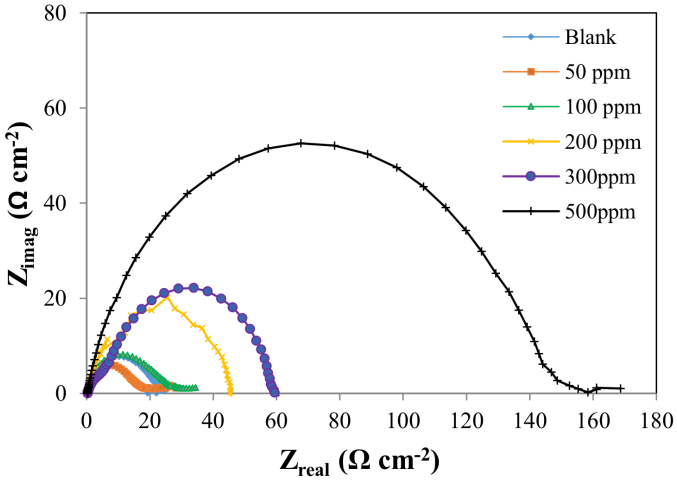

Fig. 2. Nyquist plots of API 5L X-52 steel in 2 M HCl with different concentrations of nifedipine in 2 M HCl solution

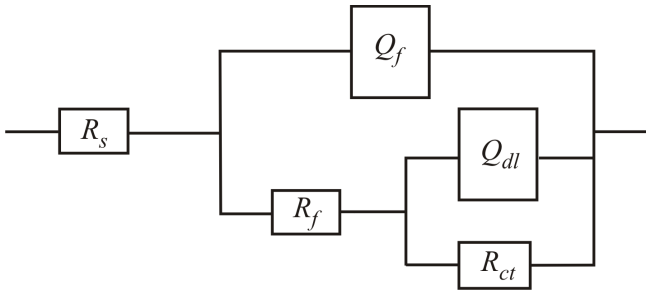

Fig. 3. Equivalent circuit for the electrochemical process at the steel surface

3.3. Adsorption isotherm

Adsorption isotherm is a model used in providing information on the interaction between the studied molecules and the metal surface. The degree of surface coverage for different concentrations of inhibitors was calculated for both measurement methods and tested on different adsorption isotherms. The experimental data fitted well using the modified Langmuir isotherm proposed by Villamil et al. [20] and given in Eq. (13);

$$\frac{C_{inh}}{\theta} = \frac{n}{K_{ads}} + nC_{inh} \tag{13}$$

where C_{inh} is the concentration of inhibitor, K_{ads} is the equilibrium constant, n the value of the slope in the Langmuir plot and θ as earlier defined. The plot of C_{inh}/θ versus C_{inh} presented in Fig. 4 gives a straight line, signifying that the adsorption of molecules under consideration on the steel surface obeys Langmuir adsorption. The free energy of adsorption ΔG_{ads} (Eq. (14)) for the corrosion of API 5L X-52 steel in 2 M HCl in the presence of the inhibitor molecule is listed in TABLE 3, including the equilibrium constant and regression coefficient.

$$K_{ads} = \frac{1}{55.5}\exp\left(\frac{-\Delta G_{ads}}{RT}\right) \tag{14}$$

where 55.5 is the concentration of water in mol/L, R is the universal gas constant in J mol^{-1} k^{-1}, T is the thermodynamic temperature in Kelvin.

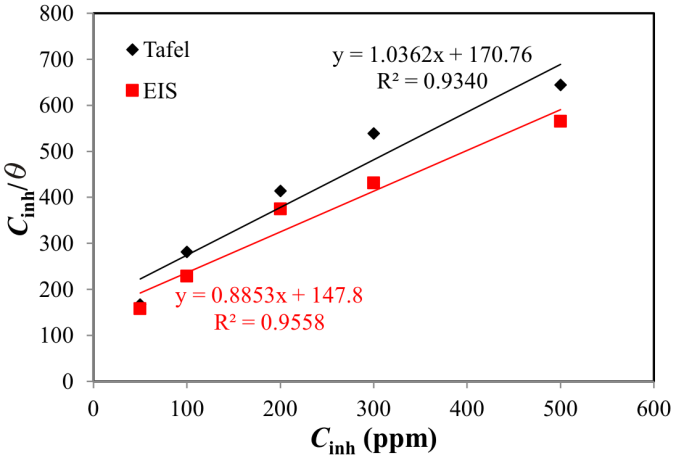

Fig. 4. Langmuir adsorption isotherm plots using Tafel and EIS results for the adsorption of nifedipine on steel in 2 M HCl

Literature [15,21] has it that if the absolute value of ΔG_{ads} is close to 20 kJ mol^{-1} or lower, the adsorption of the inhibitor mol-

TABLE 2

EIS parameters for corrosion of API 5L X-52 steel in 2 M HCl without and with different concentrations of the inhibitor molecules. R_{ct} is determined by the fit to the equivalent circuit and R'_{ct} from the difference in impedance at low and high frequencies

Inhibitor conc. (ppm)	R_s (Ω cm^2)	R_f (Ω cm^2)	Q_{dl} (S s^n cm^{-2})	n_{dl}	R_{ct} (Ω cm^2)	Q_{dl} (S s^n cm^{-2})	n_{dl}	IE (%)	R'_{ct} (Ω cm^2)	C_{dl} (mFcm^{-2})	IE' (%)
Blank	0.2064	15.310	9.513×10^{-5}	0.8952	9.07	1.352×10^{-2}	0.3901		19.24	207	
50	0.1768	11.430	6.940×10^{-5}	0.9070	19.89	5.660×10^{-2}	0.2547	54.4	28.13	142	31.6
100	0.1360	9.453	4.289×10^{-5}	0.9060	20.79	5.894×10^{-3}	0.3205	56.4	34.24	58	43.8
200	0.3288	8.745	8.876×10^{-5}	0.9780	36.75	3.757×10^{-4}	0.7712	75.3	41.30	96	53.4
300	0.3765	6.978	8.012×10^{-5}	0.9759	51.97	8.872×10^{-4}	0.8659	82.5	63.45	61	69.6
500	0.2860	2.693×10^{-6}	3.260×10^{-5}	0.9945	146.20	3.239×10^{-4}	0.7467	93.8	168.70	23	88.5

TABLE 3

Thermodynamic parameters derived from Langmuir isotherm for adsorption of nifedipine on API 5L X-52 steel in 2 M HCl at 303 K

Method	K_{ads} (×10^{-3})	R^2	ΔG_{ads} (kJ mol^{-1})
Tafel	6.07	0.934	2.74
EIS	5.99	0.956	2.77

ecules is of a physical adsorption type. This type of adsorption is linked to electrostatic interaction between charged inhibitor molecules and the charged metal. However, values close to 40 kJ mol^{-1} or higher entail a transfer of charges between the inhibitor and the metal surface reflecting chemisorption. The calculated ΔG_{ads} value for the inhibitor molecule obtained from potentiodynamic polarization and electrochemical impedance spectroscopy data are 2.74 kJ mol^{-1} and 2.77 kJ mol^{-1} respectively, indicating that physisorption mode is likely to predominate.

3.4. Statistical consideration

To compare results obtained from the two experimental measurements we adopt a statistical tool such as the T_{test} statistical model. The model was used to compare results of the two methods at concentrations of 50 ppm, 200 ppm and 500 ppm. T_{test} experimental calculated value was obtained using Eq. (15);

$$T_{test} = \frac{\bar{x}_1 - \bar{x}_2 \sqrt{\frac{MN}{M+N}}}{Sp} \tag{15}$$

where M is the number of set of values in the first method and N is the number of set of values in the second method, $\bar{x}_1$ is the mean of result of the first method while $\bar{x}_2$ is the mean of result of the second method. The pooled standard deviation Sp, was calculated using Eq. (16);

$$Sp = \sqrt{\frac{\sum_{i-1}^{M}\left(x_i - \bar{x}_1\right)^2 + \sum_{j-1}^{N}\left(x_j - \bar{x}_2\right)^2}{M+N-2}} \tag{16}$$

where x_i and x_j are the set of individual values for the first and second method respectively, M + N – 2 is the degree of freedom, df. The T_{test} experimental and critical values are listed in Table 4. The results obtained indicate that T_{test} experimental value in the two methods was found to have lower T_{test} experimental value than the critical value at significant level $\alpha = 0.005$ and degrees of freedom, $df = 4$. This means that there is no significant difference between potentiodynamic polarization method and electrochemical impedance spectroscopy method, thus suggesting a good agreement in the results obtained from the two methods.

TABLE 4

Statistical T_{test} results for the comparison of the two methods employed

Method	T_{test} experimental	Sp	T_{test} critical
Tafel & EIS	0.01	29	2.78
$\alpha = 0.005$			$df = 4$

3.5. Chemical reactivity

The chemical structure of the inhibitor molecule is presented in Fig. 5. The IUPAC name is given as 5-dimethyl-2,6-dimethyl-4-(2-nitrophenyl)-1,4-dihydropyridine-3,5-dicarboxlate and molecular formula $C_{17}H_{18}N_2O_6$ with molecular mass of 346.34 g mol^{-1}. It is an antihypertensive drug and a derivative of pyridine. The optimized structure of the compound is shown in Fig. 6. Frontier molecular orbital diagrams have also been demonstrated in Fig. 7. Quantum chemical parameters were calculated using Eq. (1)-(8) and the results are presented in Table 5.

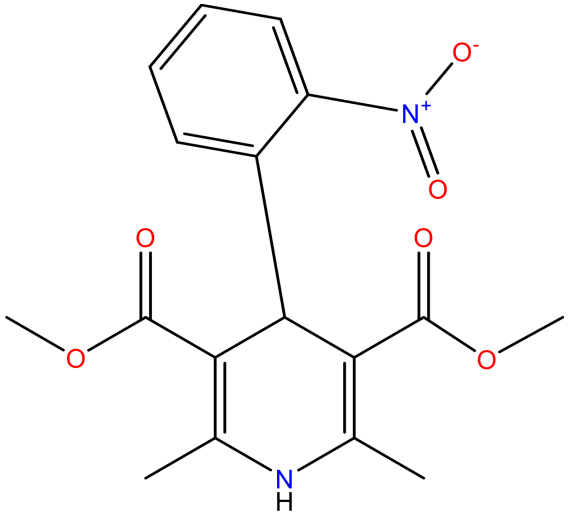

Fig. 5. Chemical structure of nifedipine

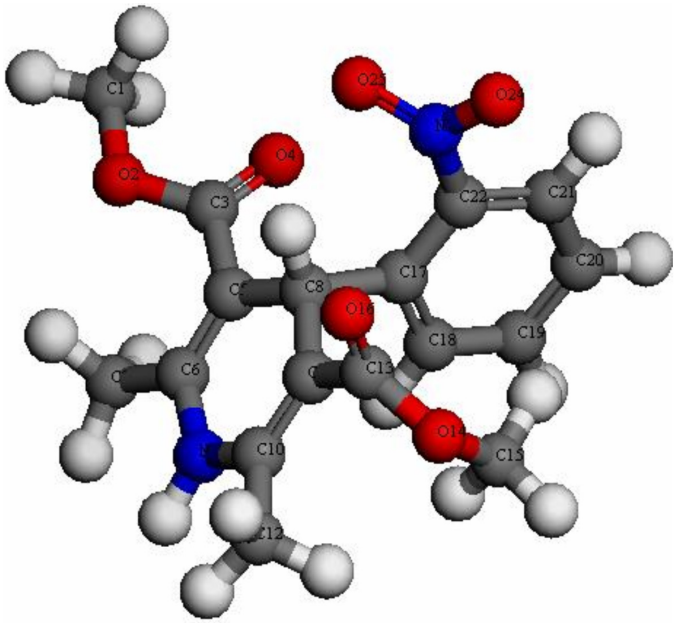

Fig. 6. Geometric optimized structure of nifedipine

TABLE 5

Quantum chemical parameters of nifedipine

E_{HOMO} (eV)	E_{LUMO} (eV)	IP (eV)	EA (eV)	ΔE (eV)	η (eV)	σ (eV^{-1})	Ω	χ (eV)	μ (debyes)
–4.386	–1.365	4.386	1.365	3.021	1.511	0.661	2.734	2.876	6.723

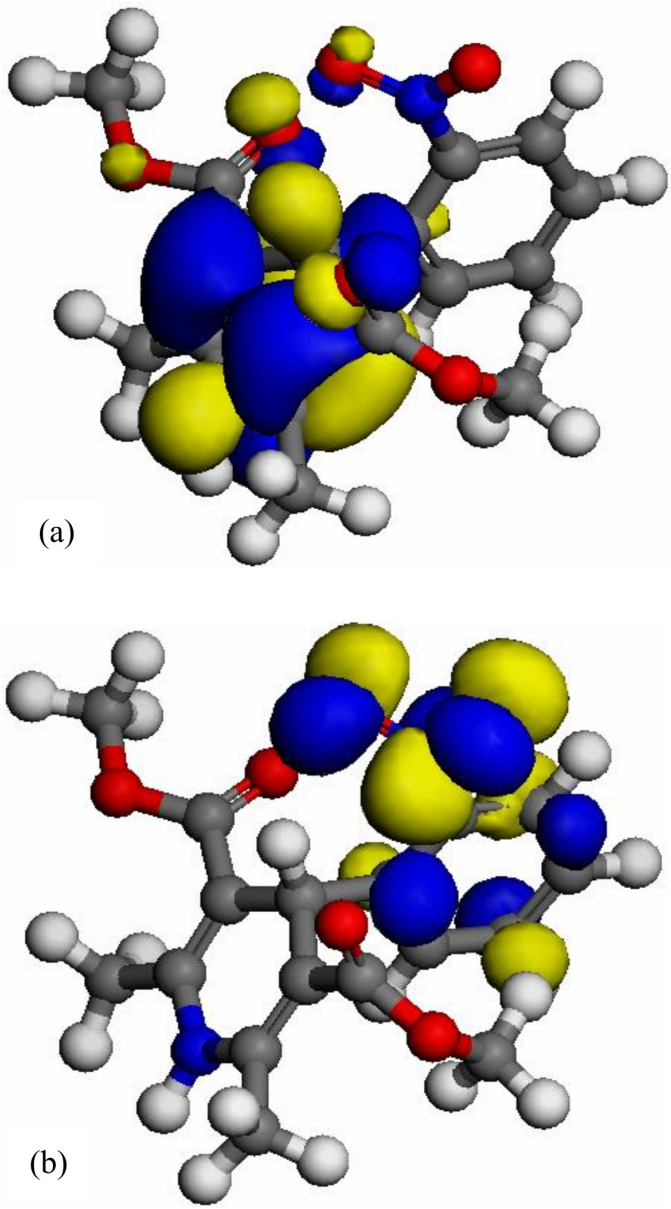

Fig. 7. Frontier molecular orbital diagrams of nifedipine molecule; (a) *HOMO* and (b) *LUMO*

In the present study, the values of the total electronic energy gives the ionization potential and electron affinity of the compound, which are related to E_{HOMO} and E_{LUMO} values respectively. As mentioned earlier, these were generated from the computational simulations. From the molecular orbital theory model, additional electrons discharged in the gaseous atom in ground electronic state as illustrated in Eq. (17) signify ionization potential and is related to E_{HOMO}.

$$H_{(g)} \rightarrow H^{+}_{(g)} + e^{-} \qquad (17)$$

Such electrons would occupy the LUMO as the electron affinity, Eq. (18);

$$Fe_{(g)} + e^{-} \rightarrow Fe^{-}_{(g)} \qquad (18)$$

The E_{HOMO} is often associated with electron donating ability of a molecule to the appropriate acceptor molecule with low energy and empty or partially filled molecular orbital. When the energy of the HOMO of a molecule is higher than the energy of the LUMO, it implies that such a molecule would have a greater tendency to facilitate adsorption and enhance inhibition efficiency [22-24]. The structural diagram of the HOMO shows a greater electron density than the LUMO, confirming electron donating ability of the molecule. Furthermore, the diagram reveals that the active centers of adsorption of the molecular specie on the surface of the steel is through nitrogen, oxygen and some carbon atoms. The importance of energy gap ΔE is also applied to predict the inhibition efficiency of a compound. ΔE is actually used to develop a theoretical model for explaining the structure and confirmation barrier in molecular systems. Therefore, the smaller the values of ΔE of a compound, the greater its inhibition efficiency. Our result for ΔE in TABLE 5 is within the recommended range of small energy gap as reported elsewhere [22,25,26]. Dipole moment is another indicator regularly used for the prediction of corrosion inhibition processes as it measures the polarity in a bond and the distribution of electrons in a molecule. Thus, molecules with high dipole moment form strong dipole-dipole interactions with metals resulting in strong adsorption onto the metal surface, leading to a greater inhibition efficiency [27]. The dipole moment obtained reveals a strong dipole-dipole interaction with the metal and is of similar range as values obtained by Elmsellem et al. [27] and Gao and Liang, [28]. A molecule with a large ΔE signifies a hard molecule and a small ΔE reflects a soft molecule. A soft molecule would easily offer electrons to an acceptor system than a hard molecule. Based on this principle, adsorption may occur at the point in a molecule where the absolute softness (σ) is high [22,27]. In other words, a molecule whose global hardness (η) is higher than global softness, illustrates the ability of a molecule to effectively inhibit the corrosion of steels. In line with the preceding argument and the results presented in Table 5, the inhibitor molecule shows tendency to suppress corrosion.

4. Conclusion

1. The molecule was found to inhibit the corrosion of API 5L X-52 steel in 2 M HCl solution. Inhibition efficiency increased with inhibitor concentration. Double layer capacitance decreased respect to the blank solution.

2. Polarization studies revealed that the inhibitor molecule functioned as a mixed-type inhibitor and the adsorption of the molecule on the steel surface obeys Langmuir isotherm model.
3. Statistical results showed that the two experimental methods employed are in good agreement with each other.
4. The study also describes the importance of quantum chemical method using Density Functional Theory in the design and selection of substances for the protection of metals in aqueous solution.

Acknowledgement

This work was supported by China-Africa Science and Technology Partnership Program (CASTEP).

REFERENCES

[1] A.L. Harvey, Drug. Discov. Today **13** (19-20), 894-901 (2008).
[2] S. Struck, U. Schmidt, B. Gruening, I. S. Jaeger, J. Hossbach, R. Preissner, Genome. Inform. **20** (231-242) (2008).
[3] https://www.caymanchem.com/msdss/11106m.pdf, accessed: 29.08.2019
[4] https://www.xenexlabs.com/wp-content/uploads/2018/06/MSDS-NN120X-NIFEDIPINE-CRYSTALLINE-POWDER-USP-1.pdf, accessed: 29.08.2019
[5] https://www.spectrumchemical.com/MSDS/N1061-AGHS.pdf, accessed: 29.08.2019
[6] G. Gece, Corros. Sci. **53** (12), 3873-3898 (2011).
[7] M.S. Morad, Corros. Sci. **50** (2), 436-448 (2008).
[8] N.O. Eddy, S.A. Odoemelam, P. Ekwumemgbo, Sci. Res. Essays **4**, 33-38 (2009).
[9] N.O. Eddy, S.A. Odoemelam, Adv. Nat. Appl. Sci. **2** (3), 225-232 (2008).
[10] A.K. Singh, E.E. Ebenso, Int. J. Electrochem. Sci. **7**, 2349-2360 (2012).
[11] M.E. Ikpi, B.O. Okonkwo, J. Mat. Environ. Sci. **8** (11), 3809-3816 (2017).
[12] F. Abeng, M. Ikpi, K. Uwakwe, G. Ikpi, Int. Res. J. P. Appl. Chem. **15** (3), 1-12 (2017).
[13] M.M. Kabanda, L.C. Murulana, M.F. Ozcan, I.D. Karadag, I.B. Obot, E.E. Ebenso, Int. J. Electrochem. Sci. **7**, 5035-5056 (2012).
[14] N.O. Obi-Egbedi, I.B. Obot, M.I. El-Khaiary, S.A. Umoren, E.E. Ebenso, Int. J. Electrochem. Sci. **6**, 5649-5675 (2011).
[15] N.O. Eddy, S.A. Odoemelam I.N. Ama, Green Chem. Lett. Rev. **3** (3), 165-172 (2010).
[16] R. Chami, M. Boudalia, S. Echihi, M. El-Fai, A. Ballouchou, A. Guenbour, M. Tabyaoui, E. M. Essassi, A. Zarrouk, Y. Ramli, J. Mat. Environ. Sci. **8** (11), 4182-4192 (2017).
[17] R. Idouhli, A.N. Ousidi, Y. Koumya, A. Abouelfida, A. Benyaich, A. Auhmani, M.Y.A. Itto, Int. J. Corros. **2018**, 1-15 (2018), DOI:10.1155/2018/9212705.
[18] I.B. Onyeachu, I.B. Obot, A.A. Sorour, M.I. Abdul-Rashid, Corros. Sci. **150**, 183-193 (2019).
[19] H. Yang, M. Zhang, A. Singh, Int. J. Electrochem. Sci. **13**, 9131-9144 (2018).
[20] R.F.V. Villamil, P. Corio, S.M.L. Agostinho, J.C. Rubim, J. Electroanal. Chem. **472**, (2) 112-119 (1999).
[21] P. Atkins, Physical Chemistry, Oxford University Press, London (1999).
[22] M.E. Ikpi, F.E. Abeng, IOP Conf. Series: Earth Environ. **173** (2018), 012018 (2018), DOI:10.1088/1755-1315/173/1/012018.
[23] M.Y. Habibat, N.O. Eddy, J.F. Iyum, C.E. Gimba, E.E. Oguzie, Chem. Mat. Res. **2** (4), 1-12 (2012).
[24] P.O. Ameh, P.U. Koha, N.O. Eddy, Chem. Sci. J. **6** (3), 100 (2015), DOI:10.4172/2150-3494.1000100.
[25] K.Y. Shalabi, Y.M. Adallah, H.M. Hassan, A.S. Fouda, Int. J. Electrochem. Sci. **9** (3), 1468-1487 (2014).
[26] A.S. Fouda, M.N. El-Haddad, Y.M. Abdallah, Int. J. Inno. Res. Sci. Eng. Tech. **2**, 7073-7085 (2013).
[27] H. Elmsellem, H. Nacer, F. Halaimia, A. Aouniti, I. Lakehal, A. Chetouani, S.S. Deyab, I. Warad, R. Touzani, B. Hammonti, Int. J. Electrochem. Sci. **9** (9), 5328 -5351 (2014).
[28] G. Gao, C. Liang, Electrochim. Acta. **52** (13), 4554-4559 (2007).